



## Evaluation of antitumor efficacy of Cerium oxide nanoparticle on Ehrlich tumour cells in mice

S.M. AbdEl-Aziz<sup>1</sup>, A.A. Baiomy<sup>2</sup>, A. B. Mansour<sup>3</sup>, R. H. Hanan<sup>4</sup>, S. A. Ali<sup>5</sup>, H. F. Attia<sup>6</sup>, Gehan B. A. Youssef<sup>7</sup>

<sup>1</sup>Faculty of Applied Health Science technology. 6th October University Egypt.

<sup>2,3,4</sup> Faculty of Science zoology Dept. Cairo University Egypt.

<sup>5</sup> Biophysics department, Faculty of Science, Cairo University, Giza, Egypt.

<sup>6,7</sup> Faculty of Veterinary Medicine Benha University Egypt.

\***Corresponding author:** Gehan B. A. Youssef, Faculty of Veterinary Medicine Benha University Egypt, Email: gihan.basiony@fvvm.bu.edu.eg

**Submitted: 11 January 2023; Accepted: 08 February 2023; Published: 06 March 2023**

---

### ABSTRACT

The goal of the current study was to assess the anticancer effects of cisplatin and cerium oxide nanoparticles on tumours caused by Ehrlich tumour cells in the skeletal muscles of female mice. The Ehrlich solid carcinoma bearing female mice were divided into 5 groups, control group Ehrlich solid carcinoma bearing mice were administered deionized dist. water for two weeks, Group 2 orally administered with ( 5% CeNPs) Group 3: orally administered with ( 10% CeNPs) Group 4: orally administered with ( 20% CeNPs) Group 5: Ehrlich solid carcinoma bearing mice were injected intra-peritoneal with Cisplatin (1 mg/kg) daily for two weeks. Antioxidant parameters, comet assay, histopathology, and mRNA expression of (P53 and K-ras ) genes were evaluated. The tumour mass was consisted of sheets and clusters of neoplastic cells with small areas of necrosis. The addition of cerium oxide nanoparticles lead to diminished the tumour masses and appearance of apoptotic holes. In the first group, the present study found higher levels of malondialdehyde (MDA) and decreased activity of the antioxidant enzymes glutathione peroxidase (GPx) and superoxide dismutase (SOD). The addition of 20% CeNPs resulted in a drop in MDA and an increase in SOD, while the activity of the GPx enzymes decreased. The K-Ras gene was up-regulated by the CeNPs, but the P53 gene was down-regulated. Cisplatin also showed similar results to cerium oxide nanoparticles but less prominent. The cerium oxide nanoparticle had antitumor efficacy as that of the cisplatin with low side effects on the tissues.

**Keywords:** *CeNPs-cisplatin. Ehrlich tumour. P-53- K-Ras- antioxidant enzymes*

## INTRODUCTION

The most prevalent rare-earth metal present in the Earth's crust is cerium, a member of the lanthanide metals with an atomic number of 58 [1]. Oxide of cerium is called ceria and has two oxidation states  $Ce^{4+}$  ( $CeO_2$ ) and  $Ce^{3+}$  ( $Ce_2O_3$ ).  $CeO_2$  has a cubic fluorite structure, where each  $Ce^{+}$  cation is surrounded by 8 oxygen anions, and each anion has a  $Ce^{+}$  tetrahedral cation [2].

The capacity of oxidation potentials and the quantity of electronegative oxygen atoms to interact with certain biomacromolecules, such as proteins, nucleic acids, and others, depends on the medium [3].

Cerium nanoparticles can interact with the free radicals that emerged from the tissues and passed the biochemical reactions cycles. It had the ability to regenerate every cycle [4].

The cerium oxide nanoparticle had the feature of catalyst [5]. It also had the feature of antioxidants and the activity of antiradicals [6]

The cerium oxide nanoparticle had the ability to created oxidative stress [7, 8]. The activity depend on the pH and the tissue environment [9].

The application of cerium oxide nanoparticles as chemotherapy for treatment of cancer because of its ability to destroy cancer cells and made it ready for radiation therapy. It also protects the surrounding normal cells from ROS and also protect the cells from its toxic effect. It considered the drug of choice for treatment of cancer [10].

Cisplatin is widely used as one of the most famous anti-cancer drugs. It was used for treatment of many types of cancer [11, 12].

Although the cisplatin had powerful effect against cancer cells but it had numerous side effects including nephrotoxicity, allergy, GIT disorders and other organs dysfunctions. The mode of action of cisplatin mainly depend on destruction of DNA repair system which lead to cell apoptosis in cancer cells. [13].

One of the most prominent disadvantage of cisplatin is induction of cytotoxicity via destruction of DNA code mechanism of replication [14]. It also activate many signalling

pathway in the tissues and activation of mitochondrial pathway [15].

## MATERIAL AND METHODS

### *Animals and ethical consideration*

Mice were obtained from National Cancer Institution (NCI) Animal house Unit. All mice have left in the animal house for one week under standard dark/light cycle to be acclimatized and supplied with standard diet pellets and water ad libitum. IACUC Protocol Number (CU I F 31 21)

### *Antitumor activity assessment*

#### *Tumor Inoculation and Grouping*

-Safety dose of Cerium oxide nanoparticles was determined to be 2000 mg/kg /b.w

- On the left hind thigh of 25 female mice, 0.2 ml of Ehrlich tumour cell suspension (containing around  $2 \times 10^6$  viable cells) would be injected intramuscularly.

- Once a solid tumour developed on day 14, mice were separated into five groups, each with five mice:

Group 1: Ehrlich solid carcinoma bearing mice were orally administered deionized dist. water for two weeks

Group 2: Ehrlich solid carcinoma bearing mice were orally administered with 5% of the determined safe dose of Cerium oxide nanoparticles daily for two weeks.

Group 3: Ehrlich solid carcinoma bearing mice were orally administered with 10% of the determined safe dose of Cerium oxide nanoparticles daily for two weeks.

Group 4: Ehrlich solid carcinoma bearing mice were orally administered with 20% of the determined safe dose of Cerium oxide nanoparticles daily for two weeks.

Group 5: Ehrlich solid carcinoma bearing mice were injected intraperitoneal with Cisplatin (1 mg/kg.bw) daily [16] for two weeks.

### *Collection of organs*

-Animals were anesthetized by using isoflurane (1-4%) and sacrificed by cervical dislocation after 24 hour of the last administration. Samples were collected from mice skeletal muscle tumor

tissues for subsequent analyses. One-half of the organs were placed in tubes containing 10% formalin for fixation and histological analysis while the other half were stored in sterilized tube at  $-80\text{ }^{\circ}\text{C}$  for later molecular assays.

#### ***Detection of DNA damage using Comet assay***

To assess the DNA damage level in tumor tissues . alkaline comet assay (Ph >13) was done according to the method described by [18 ].

#### ***Measurement of the expression level of the p53 and K-ras genes***

The expression levels of p53 and K-ras genes were measured in tumor tissues using Real Time Polymerase Chain Reaction (RT-PCR).

#### ***Extraction of whole RNA***

First whole RNA was extracted from tumor tissues using Gene JET RNA Purification Kit (Thermo scientific, USA) with the following steps:

- 1- Immersed about 30 mg of frozen tissues into liquid nitrogen and grounded it with a mortar and pestle then immediately transferred into a 1.5 mL microcentrifuge tube containing 300  $\mu\text{l}$  of Lysis Buffer supplemented with  $\beta$ - mercaptoethanol. Vortexed for 10 second and mixed thoroughly.
- 2- Added 600  $\mu\text{l}$  of diluted Proteinase K (10  $\mu\text{l}$  of the included Proteinase K diluted in 590  $\mu\text{l}$  of TE buffer), mixed by vortex and incubated at  $25^{\circ}\text{C}$  for 10 minute.
- 3- Centrifuged for 10 minute at  $12000 \times g$ , transferred the supernatant into a new RNase-free micro-centrifuge tube then added 450  $\mu\text{l}$  of ethanol (100%) and mixed by pipetting.
- 4- Transferred 700  $\mu\text{l}$  of lysate to the GeneJET RNA Purification Column inserted in a collection tube, centrifuged for 1 minute at  $12000 \times g$  then discarded the flow through.
- 5- Transferred the remaining of the lysate into the column and centrifuged. Discarded the collection tube containing the flow-through solution and the GeneJET RNA Purification Column was placed into a new 2 mL collection tube.
- 6- Added 700  $\mu\text{l}$  of Wash Buffer 1 (supplemented with ethanol) to the GeneJET RNA Purification

Column, centrifuged for 1 minute at  $12000 \times g$  and discarded the flow-through.

7- Added 600  $\mu\text{l}$  of Wash Buffer 2 (supplemented with ethanol) to the GeneJET RNA Purification Column, centrifuged for 1 minute at  $12000 \times g$  and discarded the flow through.

8- Added 250  $\mu\text{l}$  of Wash Buffer 2 to the GeneJET RNA Purification Column, centrifuged for 2 min at  $12000 \times g$ , discarded the collection tube containing the flow-through solution and transferred the GeneJET RNA Purification Column to a sterile 1.5 mL RNase-free micro-centrifuge tube

9- Added 100  $\mu\text{l}$  of nuclease-free Water to the center of the GeneJET RNA Purification Column membrane, centrifuged for 1 min at  $12000 \times g$  to elute RNA.

10- Discarded the purification and the purified RNA were stored at  $-80\text{ }^{\circ}\text{C}$  until used.

#### ***Reverse transcription of RNA***

The whole extracted RNA was converted into complementary DNA (cDNA) according to the instructions of Revert Aid First Strandc DNA Synthesis Kit (Thermo scientific, USA) as follow:

- 1- Added 5  $\mu\text{g}$  of template RNA and 1 $\mu\text{l}$  of primer to a sterile and nuclease free water to complete the final volume to 12  $\mu\text{l}$  in nuclease free tube on ice.
- 2- Added 4  $\mu\text{l}$  of 5X Reaction Buffer to 1  $\mu\text{l}$  of RiboLock RNase Inhibitor (20 U/ $\mu\text{l}$ ), 2  $\mu\text{l}$  of 10 mM dNTP and 1  $\mu\text{l}$  of Revert Aid M-MuLV RT (200 U/ $\mu\text{l}$ ) then completed the final volume to 20  $\mu\text{l}$ . Mixed gently and centrifuged briefly.
- 3- Incubated samples at  $42^{\circ}\text{C}$  for 60 minute.
- 4- Terminated the reaction by heating at  $70^{\circ}\text{C}$  for 5 minute.
- 5- Stored the reverse transcription reaction product at  $-70^{\circ}\text{C}$  until used.

#### ***Quantitative RT-PCR reaction***

Expression levels of p53 and K-ras genes were quantified via SYBR green-based real-time PCR using 7500 Fast systems (One Step Applied Biosystem 7500, Clinilab, Egypt) with the following steps.

1- Mixed 1 µl of sample cDNA with 0.5 µl of forward primer, 0.5 µl of reverse primer and 6 µl SYBER green master mix then added 4 µl of nuclease free water to complete final RT-PCR volume into 12 µl.

2- RT-PCR was started with initial denaturation 15 minute at 95°C then thirty-five cycles of denaturation at 95°C for 15 seconds, annealing at 58 for 30 second and extension at 72°C for 1 minute were performed.

3- Duplicate of each group was quantified for each gene and the results of gene expression were normalized to β actin as a housekeeping gene.

4- Gene expression was quantified using the comparative Ct (DDCt) method, as described in the Assays-On-Demand User's Manual (Applied Bio systems).

5- The fold values (x) were calculated using the formula:

$$x = 2^{(-DDCt)}$$

The DDCt was determined using the formula:

$DDC(t) = DC(t)_{treated} - DC(t)_{control}$ , Where  $DC(t)_{treated} = C(t)_{target\ gene} - C(t)_{reference\ gene}$  of the treated sample and  $DC(t)_{control} = C(t)_{target\ gene}$  of control -  $C(t)_{reference\ control}$ .

### ***Histological examination***

Small pieces of the skeletal muscle tumor from each group were collected and preserved in boiuns solution for histological analysis according to [18 ].

### ***Biochemical markers of oxidative stress assays***

These assays were conducted only tumor tissue in Antitumor activity groups Homogenates (10%) were centrifuged at 4000 rpm for 20 min. at 4°C and the supernatants were used for determination of malondialdehyde [19 ],superoxide dismutase [20]. and glutathione peroxidase activities [ 21 ].following the instructions of kits (Bio- Dignostic, Egypt).

### ***Preparation of cerium oxide nanoparticles***

Ce(III) nitrate (Ce(NO<sub>3</sub>)<sub>3</sub>. 6H<sub>2</sub>O) and Potassium carbonate K<sub>2</sub>CO<sub>3</sub> specified 99.99% pure were

purchased from Sigma-Aldrich and used without further purification. CeO<sub>2</sub> nanoparticles were synthesized using simple co-precipitation method as described in detailed [22]. The specification of the size and structure of the CeO<sub>2</sub> nanoparticles were carried out. X-ray diffractometer (XRD) was used to identify the crystalline phase and to estimate the crystalline size. The XRD pattern were recorded with 2θ in the range of 20 - 95° with type Malvern Pananalytical X-Pert Pro MPD, Cu-Kα: λ = 1.54 Å.

Using a Zetasizer Nanoseries, dynamic light scattering (DLS) was used to calculate the polydispersity (% Pd) of the distribution and the mean diameter of the CeO<sub>2</sub> nanoparticles (Malvern Instruments, UK). The sample was tested three times using the unimodal model for size distribution and the calculation factors utilised were the refractive index and viscosity of pure water. The results are provided as a mean ±SD for the polydispersity and mean diameter of the CeO<sub>2</sub> nanoparticles. At 25 °C, the size distribution was observed as a function of volume.

Zeta potential, a measurement of the electrical charge on a particle's surface, is frequently used to describe colloidal drug delivery methods. The colloidal system's potential stability is indicated by the zeta potential's magnitude. A more stable colloidal dispersion will result from more particle repulsion as the zeta potential rises. There won't be any inclination for the particles to join together if all of the particles in suspension have a strong negative or positive zeta potential [23].

### ***Statistical analysis***

All experiments were performed at least three independent times. Data shown here are presented as mean • } SE unless stated otherwise. For comparison between control and treated groups, data were analyzed by one-way analysis of variance (ANOVA) with Dunnett's multiple comparison tests using GraphPad Prism (V0.5.01). Values with P-value ≤ 0.05 were considered statistically significant.

### RESULTS

The experimental X-ray powder diffraction (XRD) pattern of the synthesized CeO<sub>2</sub> nanoparticles is shown in ( Figure 1). The characteristic peaks are very close to the fluorite structured CeO<sub>2</sub> crystal . The characteristic peaks corresponding to the (111), (200), (220), (311), (222), (400), (331), and (420) planes are located at  $2\theta = 28.55^\circ, 33.09^\circ, 47.5^\circ, 56.36^\circ, 59.1^\circ, 69.44^\circ, 76.72^\circ,$  and  $79.1^\circ$  respectively are identified using the standard data . The mean size of the CeO<sub>2</sub> nanoparticles have been estimated

from the full width at half maximum (FWHM) and Debye-Sherrer formula according to the following equation:

$$D = \frac{0.98 \lambda}{B \cos\theta}$$

Where, 0.89 is the shape factor,  $\lambda$  is the X-ray wavelength, B is the full width at half maximum (FWHM) in radians, and  $\theta$  is the Bragg angle. The mean size of the CeO<sub>2</sub> nanoparticles were determined around 25 nm.

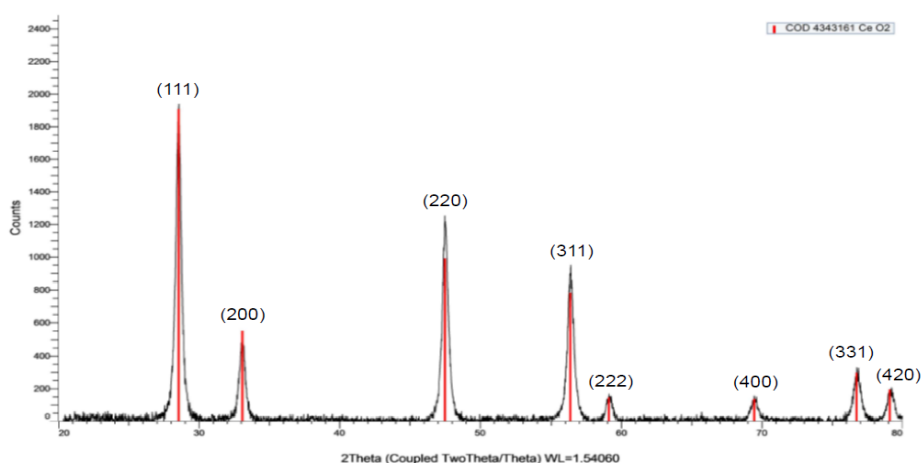


**FIGURE 1:** XRD Pattern of the CeO<sub>2</sub> nanoparticles synthesized using the coprecipitation method.

At 25 °C, the CeO<sub>2</sub> nanoparticles' DLS size distribution was unimodal and rather narrow (Figure 2 ). At 100% of the volume, the computed mean diameter was 25.02 nm. Polydispersity (%)

Pd) had a mean value of 0.330%. Thus, samples with% Pd  $\leq 20\%$  are often regarded as monodisperse.

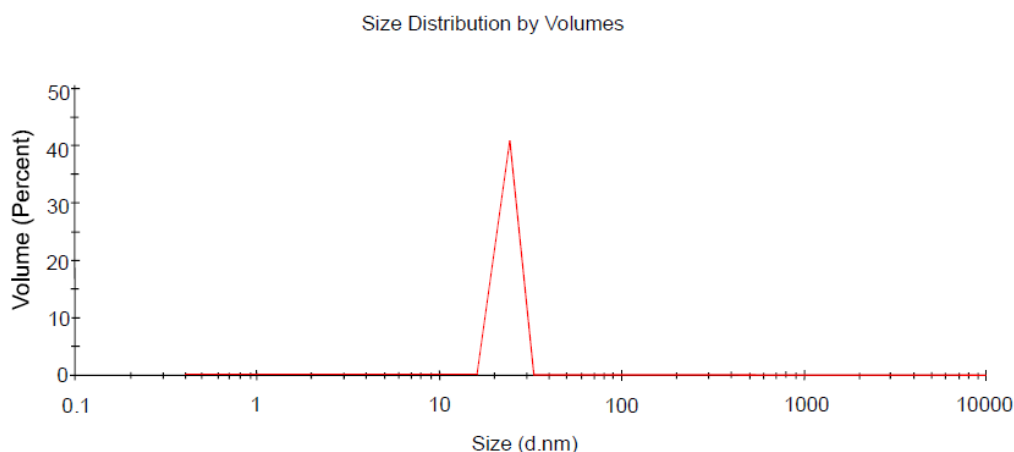


**FIGURE 2:** Size distribution measured by (DLS) of the of the CeO<sub>2</sub> nanoparticles synthesized using the coprecipitation method.

The surface potential of the synthesized CeO<sub>2</sub> nanoparticles showed a potential of 35.31 mV. The surface potential of > 25 mV along with a sharp single peak of the size distribution confirm that the CeO<sub>2</sub> nanoparticles were monodispersed and stable.

**Biochemical results**

The CeNPs showed significant decrease in MDA as shown in the table 26.0 ± 0.82 in CeNPs 5% in compare to the control group 44.0 ± 4.01 while the cisplatin and safety dose of CeNPs 20 % showed also decrease in MDA 31.0±5.78

The CeNPs showed significant increase in SOD as shown in the table 38.0 ±2.37 in CeNPs 5% in compare to the control 12.38± 1.06 while the cisplatin showed also increase in SOD 14.1±0.28. The safety dose of CeNPs 20 % showed increase in SOD 26.0± 0.87

The CeNPs showed significant decrease in Gpx as shown in the table 0.08 ± 0.03 in CeNPs 5% in compare to the control 0.69 ± 0.21 while the cisplatin showed also decrease in Gpx 0.050 ± 0.05. The safety dose of CeNPs 20 % showed decrease Gpx 0.18 ± 0.04 (Table.1 and Figure.3).

**TABLE 1:** Effect of different concentration of CeNPs and cisplatin on Biochemical parameters of oxidative stress

Biochemical parameters of oxidative stress	Tumor mass from tumor groups					F	P
	Control Mean ± SD	5% Mean ± SD	10% Mean ± SD	20% Mean ± SD	Cisplatin Mean ± SD		
SOD	12.38± 1.06	38.0 ±2.37	35.9 ± 3.13	26.0± 0.87	14.1±0.28	243.8	0.000
MDA	44.0 ± 4.01	26.0 ± 0.82	35.5 ± 2.10	31.0 ± 1.98	31.0±5.78	23.4	0.000
GPX	0.69 ± 0.21	0.08 ± 0.03	0.18 ± 0.04	0.18 ± 0.04	±0.05.00.05	31.9	0.000

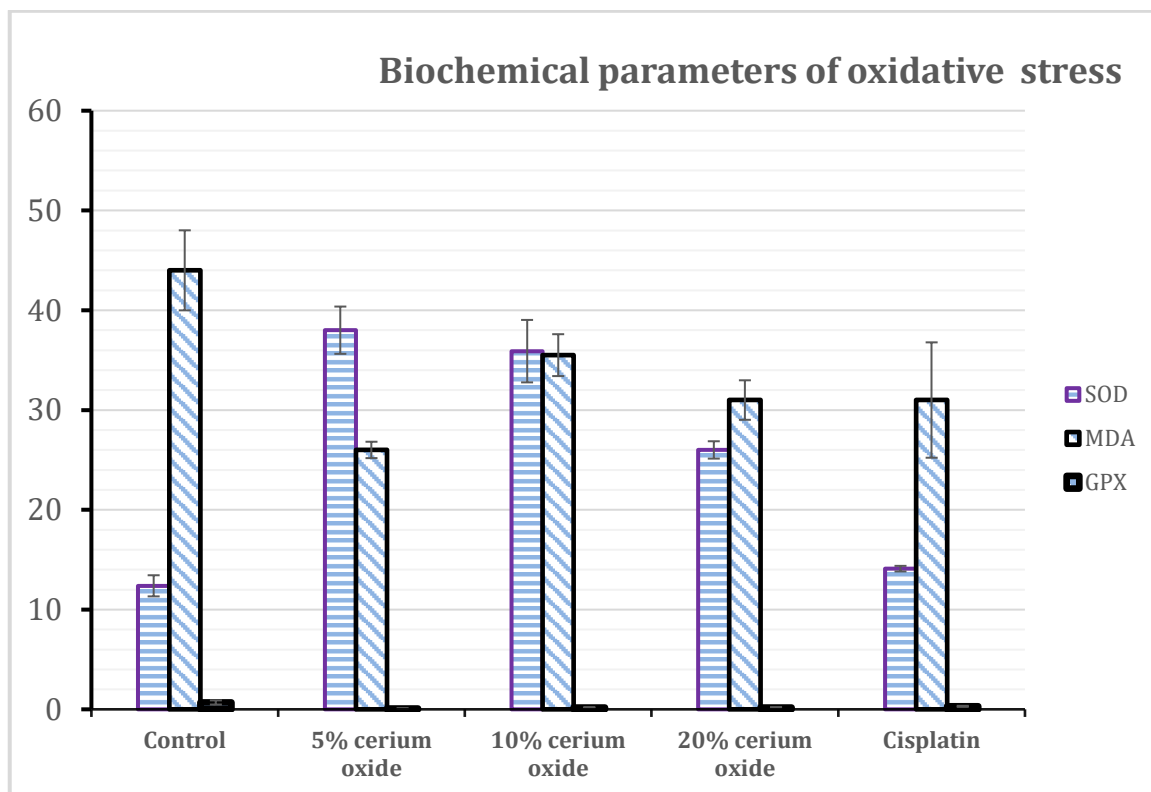


**FIGURE 3:** Effect of different concentration of CeNPs and cisplatin on Biochemical parameters of oxidative stress

**Comet assay**

The Ceo2 5% showed significant changes in tail length, % DNA and tail moment while the safety dose of CeNPs 20 % did not showed any

significant changes. The cisplatin showed less significant changes in tail length, % DNA and non-significant changes in tail moment (table2)

**TABLE 2:** Effect of different concentration of CeNPs and cisplatin on DNA damage level in tumor tissues

compounds	Tumor tissue					F	P
	Control Mean ± SD	5% Mean ± SD	10% Mean ± SD	20% Mean ± SD	Cisplatin Mean ± SD		
Length	7.91 ± 3.25	13.06 ± 0.49 a	8.00 ± 1.07	8.92 ± 2.43	10.75 ± 0.54	3.92	0.036
DNA	22.18 ± 5.29	28.58 ± 4.01	22.54 ± 1.25	27.87 ± 1.91	28.32 ± 0.21	3.18	0.062
Moment	4.45 ± 2.68	7.15 ± 0.09	3.73 ± 0.69	3.78 ± 1.31	4.77 ± 0.27	3.09	0.067

A: Significant with control group at p < 0.05

B: Significant with 5% group at p < 0.05

C: Significant with 10% group at p < 0.05

D: Significant with 20% group at p < 0.05

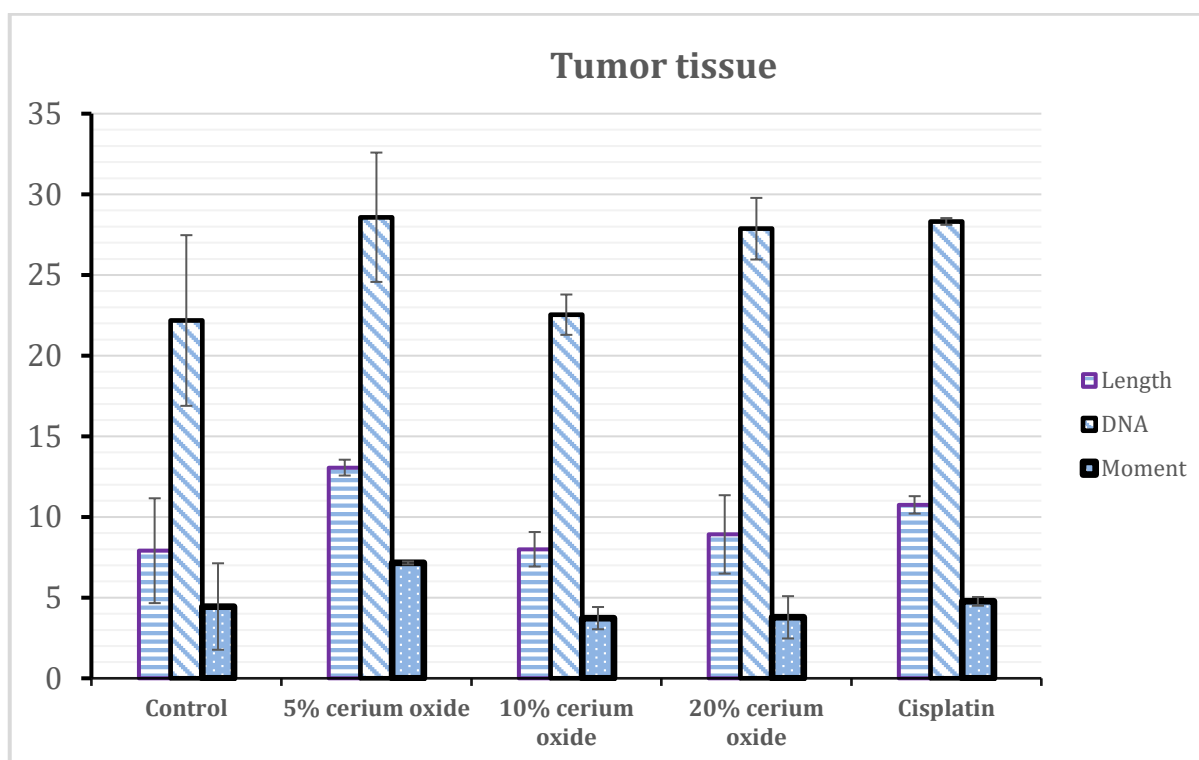


**FIGURE 4 :** Effect of different concentration of CeNPs and cisplatin on DNA damage level in tumor tissue

**Rt-PCR**

The results showed that the relative mRNA expression of P53 was significantly down-regulated. It was 1.00 ± 0.00a in cerium oxide 5%

group in comparison to control group 4.16 ± 0.17. The safety dose of CeNPs 20 % was 2.27 ± 0.28, while it was 1.98 ± 0.23 in cisplatin group.

The mRNA expressions of k-Ras was up-regulated in  $1.00 \pm 0.00$ a cerium oxide 5% group while it was  $0.44 \pm 0.05$  in cisplatin group. (table 3) in comparison to control group  $0.44 \pm 0.05$  . The

**TABLE 3:** Effect of different concentration of CeNPs and cisplatin on mRNA expressions of P53 and k-Ras

Gene	Tumor groups					F	P
	Control Mean $\pm$ SD	5% Mean $\pm$ SDa	10% Mean $\pm$ SDab	20% Mean $\pm$ SDabc	Cisplatin Mean $\pm$ SDab		
P53	$4.16 \pm 0.17$	$1.00 \pm 0.00$ a	$2.06 \pm 0.07$ ab	$2.27 \pm 0.28$ abc	$1.98 \pm 0.23$ abd	135.7	0.000
k-Ras	$0.44 \pm 0.05$	$1.00 \pm 0.00$ a	$0.75 \pm 0.04$ ab	$0.57 \pm 0.05$ ab	$0.72 \pm 0.03$ abd	78.7	0.000

A: Significant with control group at  $p < 0.05$

B: Significant with 5% group at  $p < 0.05$

C: Significant with 10% group at  $p < 0.05$

D: Significant with 20% group at  $p < 0.05$

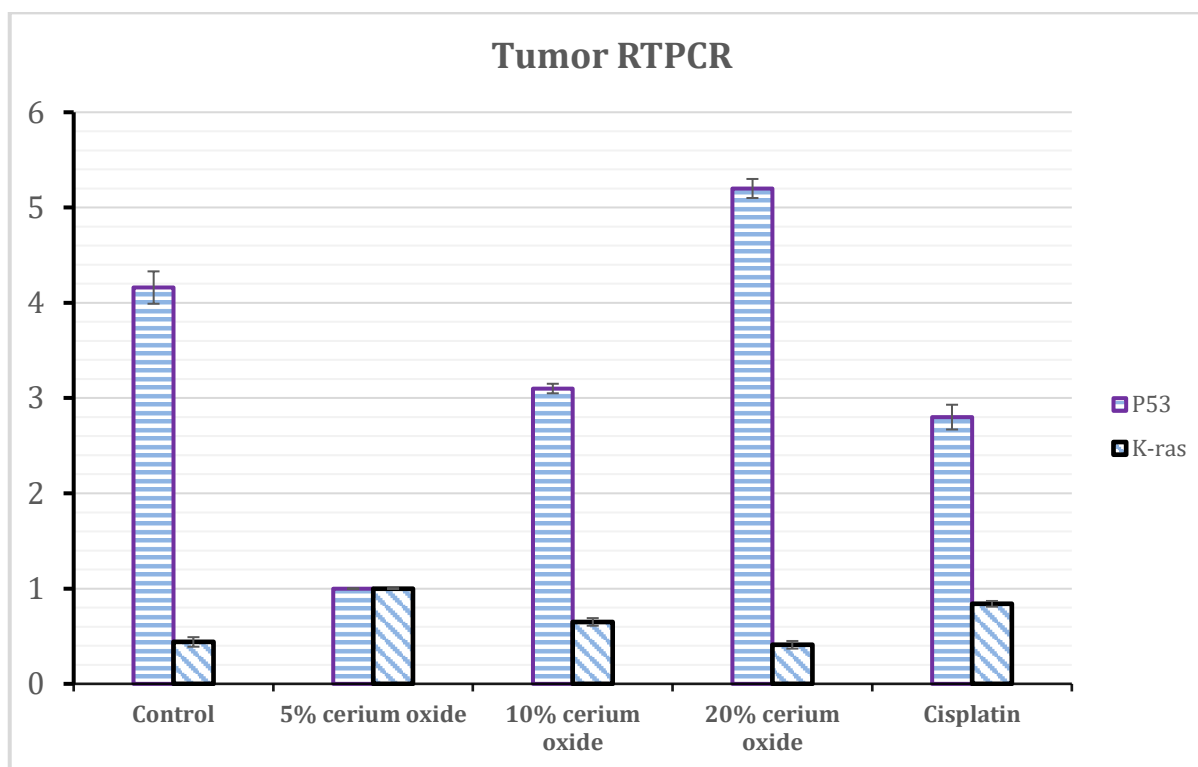


**FIGURE 5:** Effect of different concentration of CeNPs and cisplatin on mRNA expressions of P53 and k-Ras

### Histopathology

The tumor mass of control untreated group (Fig. 1-2) revealed sheets and clusters of neoplastic cells that infiltrates in-between muscle bundles. The neoplastic cells exhibited marked pleomorphism, nuclear hyperchromacia,

anisokaryosis and frequent atypical mitosis. Small focal areas of necrosis were seen in-between neoplastic cells clusters in some of the examined sections. Cerium 5% treated (Fig.3-4) exhibited mild improvement as the clusters of neoplastic cells were existing with development

of few apoptotic holes and areas of necrosis within. The frequency of mitosis was slightly lowered. Regarding Cerium 10% treated group (Fig. 5-6) the solid carcinoma masses were decreased in size with increased area of necrosis within the tumor cells clusters. Numerous apoptotic holes were seen within the neoplastic cells with marked reduction in mitotic figures. Marked improvement was noticed in Cerium 20% treated group (Fig. 7-8), the tumor masses were decreased in size with diffuse necrosis in

neoplastic cells. The mitotic frequency was markedly reduced in the remnant neoplastic cells. Some of the examined sections revealed few neoplastic cells within apparently healthy muscle bundles. Cisplatin treated group (Fig. 9-10) showed marked improvement as well. The neoplastic cells were replaced by wide areas of necrosis with marked reduction in tumor cells density. The mitosis frequency was greatly reduced.

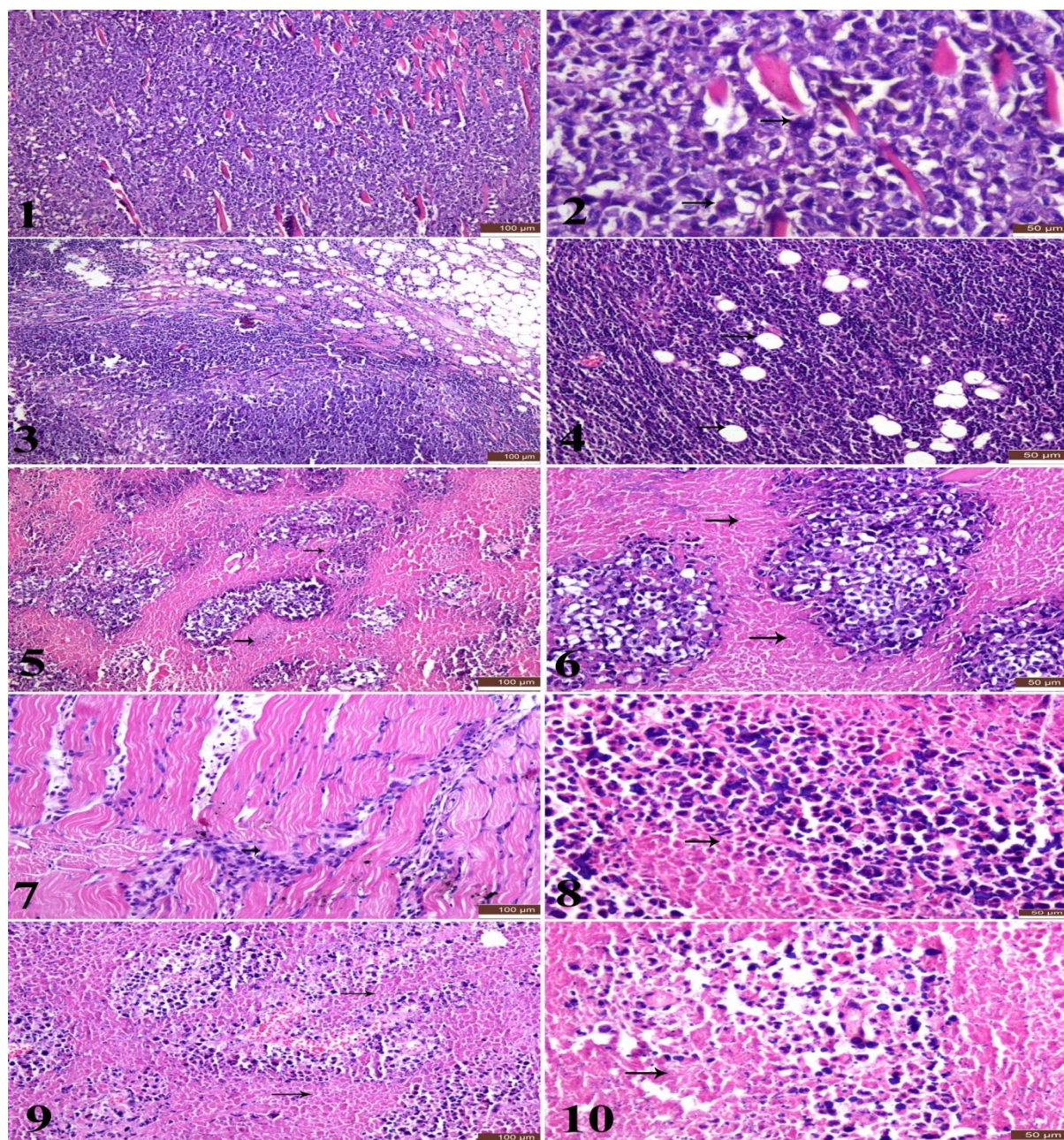


**FIG. (1)** Photomicrograph of Ehrlich tumor mass, Control untreated group showing sheet of neoplastic cells infiltrating between muscles (H&E).

**FIG. (2)** Photomicrograph of Ehrlich tumor mass, Control untreated group higher magnification showing marked pleomorphism and frequent mitosis (arrows) in neoplastic cells (H&E).

**FIG. (3)** Ehrlich tumour mass photomicrograph, Cerium 5% treated group, displaying clusters of malignant cells in between muscle bundles (H&E).

**FIG. (4)** Photomicrograph of Ehrlich tumor mass, Cerium 5% treated group showing clusters of neoplastic cells with some apoptotic spaces (arrows) within (H&E).

**FIG. (5)** Photomicrograph of Ehrlich tumor mass, Cerium 10% treated group showing wide areas of necrosis (arrows) with decreased neoplastic cells masses (H&E).

**FIG. (6)** Photomicrograph of Ehrlich tumor mass, Cerium 10% treated group higher magnification showing wide areas of necrosis with decreased neoplastic cells mass (arrows) (H&E).

**FIG. (7)** Photomicrograph of Ehrlich tumor mass, Cerium 20% treated group higher magnification showing few neoplastic cells (arrows) in-between muscle bundles (H&E).

**FIG. (8)** Photomicrograph of Ehrlich tumor mass, Cerium 20% treated group showing diffuse necrosis within neoplastic cells (arrows) with less frequent mitosis (H&E).

**FIG. (9)** Photomicrograph of Ehrlich tumor mass, Cisplatin treated group higher wide area of necrosis (arrows) with few neoplastic cells (H&E).

**FIG. (10)** Photomicrograph of Ehrlich tumor mass, Cisplatin treated group higher magnification showing wide area of necrosis with few neoplastic cells (arrows) (H&E).

## DISCUSSION

Lipid peroxidation (LPO) necessitates the oxidative degradation of polyunsaturated fatty acids (PUFA), which modifies the structure and operation of membranes. This calls for a decrease in membrane fluidity and the deactivation of membrane-bound enzymes [24]. The earliest defence against oxidative stress brought on by ROS is thought to be the SOD and GPx [25]. Cell damage might result from the ROS generation's impact on mitochondrial performance and lipid peroxidation (MDA) levels [26].

Our findings were reported that the cerium oxide nanoparticles had antioxidants effect against the tissue hazard caused by the induced tumour. The cerium oxide nanoparticles decreased the MDA and increased the antioxidant enzyme SOD although the GPx not increased. These findings also supported by the results of cisplatin group but the intensity of results were directed toward the cerium oxide nanoparticles. These results were augmented by [27] although these authors showed increase in GPx antioxidant

Although the cisplatin is used as chemotherapy in the treatment of cancer that had excellent penetration power [28] but it had numerous side

effects [29] that lead the pharmacist to search for another substitutes that had low tissue toxicity [30]. The cisplatin accumulation encourages cellular apoptosis and cytotoxicity [31,32].

In contrast to our work that cisplatin decreased MDA and increased SOD and showed improvements in histopathological alteration in the tumour skeletal muscle [33] showed increased MDA and decreased SOD and Gpx. Cisplatin also accelerated the cells to undergoes apoptotic pathway [34].

Owing to the industry's extensive usage of cerium oxide nanoparticles [CeO<sub>2</sub> NPs; nanoceria (NC)] and their employment in biology and medicine, researchers have lately been interested in examining their antioxidant qualities. [35]. According to [36] NC with free radical scavenging has a protective effect against oxidative stress. This element's antioxidant actions prevent apoptosis coupled with a decrease in the buildup of reactive oxygen species (ROS) [37]. One of the most significant types of nanomaterials, NC, has the potential to undergo redox reactions.

Not only cerium oxide nanoparticles but all the nanoparticles have the ability to have antioxidant

activity and deal with ROS [38]. It also can overcome the disorders or diseases [39].

The cerium oxide nanoparticle may have anti-invasive character against some cancer cells [40], induces radio-sensitisation [41], and simultaneously radioprotection of normal cells by regulating antioxidant enzymes and quantity of ROS [32, 42]. It has low cytotoxic effect against human cancer cells [43]

According to our findings, P53's relative mRNA expression was dramatically down-regulated. It was  $1.00 \pm 0.00a$  in cerium oxide 5% group in comparison to control group  $4.16 \pm 0.17$ . The safety dose of CeNPs 20% was  $2.27 \pm 0.28$ , while it was  $1.98 \pm 0.23$  in cisplatin group.

P53 protein, one of the most important tumor suppressor proteins, is often abnormally expressed in most human tumors [44]

When the expression of P53 was up-regulated the induction of ROS was increased so the ROS is considered one of the initiator of apoptosis in the cells [45]

Cerium oxide down-regulated the mRNA of P53 in our current work while [46] showed that the cerium oxide may activate the P53 and induce apoptosis

Cisplatin made direct inactivation of P53 and interfere with the DNA of the cells via formation of cross link and directly decreased apoptosis [47,48] who support that cisplatin made P53 stabilization in the cells.

Our results showed that the mRNA expressions of k-Ras was up-regulated in  $1.00 \pm 0.00a$  cerium oxide 5% group in comparison to control group  $0.44 \pm 0.05$ . The safety dose of CeNPs 20% was  $0.57 \pm 0.05ab$  while it was  $0.44 \pm 0.05$  in cisplatin group. Structure, localization, and function of the KRAS protein. KRAS is a member of the RAS superfamily, also known as the RAS-like GTPases, which is a subset of small GTP-binding proteins. In mammalian genomes, more than 150 RAS-like genes have been discovered [49]. Activation of K-ras or upregulation of mRNA of K-Ras means that tissue is fastly subjected to death and had poor response to the treatment with the chemotherapy [50].

## REFERENCES

1. Dahle J. T. and Y. Arai, Environmental Geochemistry of Cerium: Applications and Toxicology of Cerium Oxide Nanoparticles. *Int. J. Environ. Res. Public Health*, 2015, 12, 1253–1278. <https://doi.org/10.3390/ijerph120201253>
2. Charbgo F., M. Ramezani and M. Darroudi, *Biosens. Bioelectron.*, 2017, 96, 33–43. doi: 10.1016/j.bios.2017.04.037. Epub 2017 Apr 26.
3. Chetty R. and M. Singh, In-vitro interaction of cerium oxide nanoparticles with hemoglobin, insulin, and dsDNA at 310.15 K: Physicochemical, spectroscopic and in-silico study. *Int. J. Biol. Macromol.*, 2020, 156, 1022–1044. DOI: 10.1016/j.ijbiomac.2020.03.067
4. Zhang F, P. Wang, J. Koberstein, S. Khalid, S.W. Chan, Cerium oxidation state in ceria nanoparticles studied with X-ray photoelectron spectroscopy and absorption near edge spectroscopy, *Surf. Sci.* 563 (2004) 74–82. <https://doi.org/10.1016/j.susc.2004.05.138>
5. Rzigalinski B.A., K. Meehan, R.M. Davis, Y. Xu, W.C. Miles, C.A. Cohen, *Radical nanomedicine, Nanomedicine (Lond.)* 1 (2008) 399–412. DOI: 10.2217/17435889.1.4.399
6. Schubert, D. R. Dargusch, J. Raitano, S. Chan, Cerium and yttrium oxide nanoparticles are neuroprotective, *Biochem. Biophys. Res. Commun.* 32 (2006) 86–91. DOI: 10.1016/j.bbrc.2006.01.129
7. Park E.J., J. Choi, Y.K. Park, K. Park, Oxidative stress induced by cerium oxide nanoparticles in cultured BEAS-2B cells, *Toxicology* 245 (2008) 90–100. DOI: 10.1016/j.tox.2007.12.022
8. Hamrahi-Michak M, S.A. Sadeghi, H. Haghighi, Y. Ghanbari-Kakavandi, S.A. Razavi-sheshdeh, M. Torkamani Noughabi, M. Negahdary, The toxicity effect of cerium oxide nanoparticles on blood cells of male rat, *Ann. Biol. Res.* 3 (2012) 2859–2866. DOI: 10.1016/j.cbi.2015.03.013
9. Asati A, S. Santra, C. Kaittanis, J.M. Perez, Surface-charge-dependent cell localization and cytotoxicity of cerium oxide nanoparticles, *ACS Nano* 4 (2010) 5321–5331. DOI: 10.1021/nn100816s
10. Ying Gao, Kan Chen, Jin-lu Ma, and Fei Gao, Cerium oxide nanoparticles in cancer. *Oncotargets Ther.* 2014; 7: 835–840. doi: 10.2147/OTT.S62057
11. Rosenberg, B, In *Nucleic Acid-Metal Ion Interactions*; Spiro, T.G., Ed.; John Wiley & Sons, Inc.: New York, NY, USA, 1980; Volume 1, pp. 1–29.
12. Desoize, B.; Madoulet, C, Particular aspects of platinum compounds used at present in cancer treatment. *Crit. Rev. Oncol. Hematol.* 2002, 42, 317–325. DOI: 10.1016/s1040-8428(01)00219-0
13. Shaloam Dasari 1, Paul Bernard Tchounwou, Cisplatin in cancer therapy: molecular mechanisms of action *J. Epub* 2014.07.025.

- 2014 Jul 21. DOI: 10.1016/j.ejphar.2014.07.025
14. Sumit Ghosh, Cisplatin: The first metal based anticancer drug. *j.bioorg.*2019.102925. Epub 2019 Apr 11. DOI: 10.1016/j.bioorg.2019.102925
  15. Ana-Maria Florea and Dietrich Büsselberg, Cisplatin as an Anti-Tumor Drug: Cellular Mechanisms of Activity, Drug Resistance and Induced Side Effects. *Cancers* 2011, 3, 1351-1371; doi:10.3390/cancers3011351
  16. Chen, Y., Han, F., Cao, L. H., Li, C., Wang, J. W., Li, Q. & Zhou, J. H, Dose-response relationship in cisplatin-treated breast cancer xenografts monitored with dynamic contrast-enhanced ultrasound. *BMC cancer*, 2015.15(1), 1-9. doi: 10.1186/s12885-015-1170-8
  17. Tice, R. R., Agurell, E., Anderson, D., Burlinson, B., Hartmann, A., Kobayashi, H., & Sasaki, Y. F, Single cell gel/comet assay: guidelines for in vitro and in vivo genetic toxicology testing. *Environmental and molecular mutagenesis*, 2000.35(3), 206-221. doi: 10.1002/(sici)1098-2280(2000)35:3<206::aid-em8>3.0.co;2-j.
  18. Bancroft, J. D., and Layton, C, "The hematoxylin and eosin, connective and mesenchymal tissues with their stains," in *Bancroft's Theory and Practice of Histological Techniques*, eds K. S. Suvarna, C. Layton, and J. D. Bancroft (Philadelphia, PA: Churchill Livingstone), 2013. 173-186.
  19. Ohkawa, H., Ohishi, N., & Yagi, K, Assay for lipid peroxides in animal tissues by thiobarbituric acid reaction. *Analytical biochemistry*, 1979. 95(2), 351-358.
  20. Abdel-Mawla, M. Y., Nofal, E., Khalifa, N., Abdel-Shakoor, R., & Nasr, Role of oxidative stress in psoriasis: An evaluation study. *J Am Sci*, 2013. 9, 151-5. <http://www.jofamericanscience.org>.
  21. Paglia, D. E., & Valentine, W. N. (1967). Studies on the quantitative and qualitative characterization of erythrocyte glutathione peroxidase. *The Journal of laboratory and clinical medicine*, 70(1), 158-169. PMID: 6066618
  22. Farahmandjou, M., Zarinkamar, M., Firoozabadi, T. P, Synthesis of Cerium Oxide (CeO<sub>2</sub>) nanoparticles using simple CO-precipitation method. *Rev. Mex. Fis.* 2016. 62, 496-499
  23. Paolino D, Fresta M, Sinha P, Ferrari M, Drug delivery systems. In: Webster JG, editor. *Encyclopedia of medical devices and instrumentation*. 2nd ed. John Wiley and Sons; 2006. p. 437-95.
  24. Gutteridge, J. M., and Halliwell, B, Free radicals and antioxidants in the year 2000: a historical look to the future. *Ann. N. Y. Acad. Sci.* 899, 136-147. doi: 10.1111/j.1749-6632.2000.tb06182.x
  25. Ighodaro, O., and Akinloye, O, First line defence antioxidants-superoxide dismutase (SOD), catalase (CAT) and glutathione peroxidase (GPX): their fundamental role in the entire antioxidant defence grid. *Alexandria J. Med.* 54, 2018.287-293. doi: 10.1016/j.ajme.2017.09.001
  26. Chen, Q., Niu, Y., Zhang, R., Guo, H., Gao, Y., Li, Y., et al, The toxic influence of paraquat on hippocampus of mice: involvement of oxidative stress. *Neurotoxicology* 31, 310-316. doi: 10.1016/j.neuro.2010.02.006
  27. Elshony Norhan, Atef M. K. Nassar, Yasser S. El-Sayed, Dalia Samak,
  28. Ahmed Noreldin, Lamiaa Wasef, Hamida Saleh, Yaser H. A. Elewa, Shereen E. Tawfeek, Abdullah A. Saati, Gaber, Ameliorative Role of Cerium Oxide Nanoparticles Against Fipronil Impact on Brain Function, Oxidative Stress, and Apoptotic Cascades in Albino Rats. *Frontiers in Neuroscience* | [www.frontiersin.org](http://www.frontiersin.org) 2 May 2021 | Volume 15. DOI: 10.3389/fnins.2021.651471
  29. Dasari, S., and Tchounwou, P. B, Cisplatin in cancer therapy: molecular mechanisms of action. *Eur. J. Pharmacol.* 740, 364-378. doi:10.1016/j.ejphar. 2014.07.025
  30. Prasad R and SB Prasad, Histoprotective effect of rutin against cisplatin-induced toxicities in tumor-bearing mice: Rutin lessens cisplatin-induced toxicities. *Human and Experimental Toxicology* 2021, Vol. 40(2) 245-258. DOI: 10.1177/0960327120947793
  31. Barabas, K., Milner, R., Lurie, D., and Adin, C, Cisplatin: a review of toxicities and therapeutic applications. *Vet. Comp. Oncol.*, 2008. 6 (1), 1. doi:10.1111/j.1476-5829.2007.00142.x
  32. Omar, H. A., Mohamed, W. R., Arab, H. H., and Arafa, E.-S. A, Tangeretin alleviates cisplatin-induced acute hepatic injury in rats: targeting MAPKs and apoptosis. *PLoS One* 2016. 11 (3), doi:10.1371/journal.pone.0151649
  33. Qi, L., Luo, Q., Zhang, Y., Jia, F., Zhao, Y., and Wang, F, Advances in toxicological research of the anticancer drug cisplatin. *Chem. Res. Toxicol.* 2019.32 (8), 1469-1486. DOI: 10.1021/acs.chemrestox.9b00204
  34. Abouzeinab, N. S, Antioxidant effect of silymarin on cisplatin-induced renal oxidative stress in rats. *J Pharmacol Toxicol*, 2015. 10(1), 1-19. DOI: 10.3923/jpt.2015.1.19
  35. Karakoc, H. T., Altintas, R., Parlakpınar, H., Polat, A., Samdanci, E., Sagir, M., & Duran, Z. R, Protective Effects of Molsidomine Against Cisplatin-Induced Nephrotoxicity. *Advances in clinical and experimental medicine: official organ Wroclaw Medical University*, 2015.24(4), 585-593. doi: 10.17219/acem/47742
  36. Colon J, N. Hsieh, A. Ferguson, P. Kupelian, S. Seal, D.W. Jenkins, C.H. Baker, Cerium oxide nanoparticles protect gastrointestinal epithelium from radiation-induced damage by reduction of reactive oxygen species and upregulation of

- superoxide dismutase 2, *Nanomedicine* 6 (2010) 698–705. DOI: 10.1016/j.nano.2010.01.010
37. Kong L, Cai X, Zhou X, Wong LL, Karakoti AS, Seal S, et al, Nanoceria extend photoreceptor cell lifespan in tubby mice by modulation of apoptosis/survival signaling pathways. *Neurobiol Dis* 2011; 42(3): 514-23. DOI: 10.1016/j.nbd.2011.03.004
  38. Giri S, Karakoti A, Graham RP, Maguire JL, Reilly CM, Seal S, et al, Nanoceria: a rare-earth nanoparticle as a novel anti-angiogenic therapeutic agent in ovarian cancer. *PLoS One* 2013; 8(1). <https://doi.org/10.1371/journal.pone.0054578>
  39. Waris G, H. Ahsan, Reactive oxygen species: role in the development of cancer and various chronic conditions, *J. Carcinog.* 5 (2006) 14. doi: 10.1186/1477-3163-5-14
  40. Elswaifi S.F., J.R. Palmieri, K.S. Hockey, B.A. Rzigalinski, Antioxidant nanoparticles for control of infectious disease, *Infect. Disord. Drug Targets* 9 (2009) 445–452. DOI: 10.2174/187152609788922528
  41. Alili L, M. Sack, A.S. Karakoti, S. Teuber, K. Puschmann, S.M. Hirst, C.M. Reilly, K. Zanger, W. Stahl, S. Das, S. Seal, P. Brenneisen, Combined cytotoxic and anti-invasive properties of redox active nanoparticles in tumor–stroma interactions, *Biomaterials* 32 (2011) 2918–2929. DOI: 10.1016/j.biomaterials.2010.12.056
  42. Wason M.S, J. Colon, S. Das, S. Seal, J. Turkson, J. Zhao, C.H. Baker, Sensitization of pancreatic cancer cells to radiation by cerium oxide nanoparticle-induced ROS production, *Nanomedicine* 9 (2013) 558–569. DOI: 10.1016/j.nano.2012.10.010
  43. Madero-Visbal R.A, B.E. Alvarado, J.F. Colon, C.H. Baker, M.S. Wason, B. Isley, S. Seal, C.M. Lee, S. Das, R. Manon, Harnessing nanoparticles to improve toxicity after head and neck radiation, *Nanomedicine* 8 (2012) 1223–1231. DOI: 10.1016/j.nano.2011.12.011
  44. Milica Pešić , Ana Podolski-Renić , Sonja Stojković , Branko Matović , Danica Zmejkoski , Vesna Kojic , Gordana Bogdanović , Aleksandra Pavićević , Miloš Mojović , Aleksandar Savic , Ivana Milenković , Aleksandar Kalauzi , Ksenija Radotić , Anti-cancer effects of cerium oxide nanoparticles and its intracellular redox activity. *Chemico-Biological Interactions* 232 (2015) 85–93. <https://www.researchgate.net/deref/http%3A%2F%2Fdx.doi.org%2F10.1016%2Fj.cbi.2015.03.013>
  45. Wang, J., Yang, W., He, X., Zhang, Z., & Zheng, X, Assembling p53 activating peptide with CeO2 nanoparticle to construct a metallo-organic supermolecule toward the synergistic ferroptosis of tumor. *Frontiers in Bioengineering and Biotechnology*, 2022.10. <https://doi.org/10.3389/fbioe.2022.929536>
  46. Polyak K, Xia Y, Zweier JL, Kinzler KW, Vogelstein B 1997. A model for p53-induced apoptosis. *Nature (Lond.)* 1997;389:300 –5. DOI: 10.1038/38525
  47. Mittal, S., & Pandey, A. K, Cerium oxide nanoparticles induced toxicity in human lung cells: role of ROS mediated DNA damage and apoptosis. *BioMed research international*, 2014. DOI: 10.1155/2014/891934
  48. Tan, M., Toplu, Y., Varan, E., Sapmaz, E., Özhan, O., Parlakpınar, H., & Polat, A, The effect of genistein on cisplatin induced ototoxicity and oxidative stress. *Brazilian Journal of Otorhinolaryngology*, 2022.88, 105-111. DOI: 10.1016/j.bjorl.2021.07.001
  49. Shin, J. N., Seo, Y. W., Kim, M., Park, S. Y., Lee, M. J., Lee, B. R., ... & Kim, T. H, Cisplatin inactivation of caspases inhibits death ligand-induced cell death in vitro and fulminant liver damage in mice. *Journal of Biological Chemistry*, 2005. 280(11), 10509-10515. DOI: 10.1074/jbc.M413865200
  50. Wennerberg, K., Rossman, K. L., & Der, C. J, The Ras superfamily at a glance. *Journal of cell science*, 2005.118(5), 843-846. DOI: 10.1242/jcs.01660
  51. Jančík, S., Drábek, J., Radzioch, D., & Hajdúch, M, Clinical relevance of KRAS in human cancers. *Journal of Biomedicine and Biotechnology*, 2010. DOI: 10.1155/2010/150960